

JGR Atmospheres

RESEARCH ARTICLE

10.1029/2022JD037257

Key Points:

- We present an updated representation of aromatic organic aerosol (OA) formation incorporating advances in interpreting chamber experiments
- Our model's improved scheme is better able to simulate OA observed during the Korea-United States Air Quality Study field campaign
- Surface OA in South Korea has on average one third each domestic anthropogenic, external anthropogenic, and natural origins

Supporting Information:

Supporting Information may be found in the online version of this article.

Correspondence to:

J. F. Brewer,
brew222@umn.edu

Citation:











Brewer, J. F., Jacob, D. J., Jathar, S. H., He, Y., Akherati, A., Zhai, S., et al. (2023). A scheme for representing aromatic secondary organic aerosols in chemical transport models: Application to source attribution of organic aerosols over South Korea during the KORUS-AQ campaign. *Journal of Geophysical Research: Atmospheres*, 128, e2022JD037257. <https://doi.org/10.1029/2022JD037257>

Received 6 JUN 2022
Accepted 21 MAR 2023

Author Contributions:

Conceptualization: J. F. Brewer, D. J. Jacob, S. H. Jathar, A. Akherati, D. S. Jo, A. Hodzic, J. L. Jimenez, R. J. Park, Y. J. Oak
Data curation: J. F. Brewer, B. A. Nault, P. Campuzano-Jost, J. L. Jimenez, R. J. Park, Y. J. Oak, H. Liao
Formal analysis: J. F. Brewer
Investigation: S. Zhai, B. A. Nault
Methodology: J. F. Brewer, S. H. Jathar, Y. He, A. Akherati, S. Zhai, D. S. Jo, A. Hodzic, Y. J. Oak
Resources: D. J. Jacob
Software: J. F. Brewer, S. Zhai, D. S. Jo, A. Hodzic
Supervision: D. J. Jacob

A Scheme for Representing Aromatic Secondary Organic Aerosols in Chemical Transport Models: Application to Source Attribution of Organic Aerosols Over South Korea During the KORUS-AQ Campaign

J. F. Brewer^{1,2} , D. J. Jacob¹, S. H. Jathar³ , Y. He³, A. Akherati^{3,4} , S. Zhai¹, D. S. Jo⁵ , A. Hodzic⁵ , B. A. Nault⁶, P. Campuzano-Jost^{7,8} , J. L. Jimenez^{7,8} , R. J. Park⁹ , Y. J. Oak⁹ , and H. Liao¹⁰ 

¹Harvard John A. Paulson School of Engineering and Applied Sciences, Harvard University, Cambridge, MA, USA, ²Department of Soil, Water, and Climate, University of Minnesota, St. Paul, MN, USA, ³Department of Mechanical Engineering, Colorado State University, Ft. Collins, CO, USA, ⁴Department of Atmospheric Sciences, Colorado State University, Ft. Collins, CO, USA, ⁵National Center for Atmospheric Research (NCAR), Boulder, CO, USA, ⁶Center for Aerosol and Cloud Chemistry, Aerodyne Research, Billerica, MA, USA, ⁷Department of Chemistry, University of Colorado, Boulder, CO, USA, ⁸Cooperative Institute for Research in Environmental Sciences, University of Colorado, Boulder, CO, USA, ⁹School of Earth and Environmental Sciences, Seoul National University, Seoul, Republic of Korea, ¹⁰Jiangsu Key Laboratory of Atmospheric Environment Monitoring and Pollution Control, Collaborative Innovation Center of Atmospheric Environment and Equipment Technology, School of Environmental Science and Engineering, Nanjing University of Information Science and Technology, Nanjing, China

Abstract We present a new volatility basis set (VBS) representation of aromatic secondary organic aerosol (SOA) for atmospheric chemistry models by fitting a statistical oxidation model with aerosol microphysics (SOM-TOMAS) to results from laboratory chamber experiments. The resulting SOM-VBS scheme also including previous work on SOA formation from semi- and intermediate volatile organic compounds (S/IVOCs) is implemented in the GEOS-Chem chemical transport model and applied to simulation of observations from the Korea-United States Air Quality Study (KORUS-AQ) field campaign over South Korea in May–June 2016. Our SOM-VBS scheme can simulate the KORUS-AQ organic aerosol (OA) observations from aircraft and surface sites better than the default schemes used in GEOS-Chem including for vertical profiles, diurnal cycle, and partitioning between hydrocarbon-like OA and oxidized OA. Our results confirm the important contributions of oxidized primary OA and aromatic SOA found in previous analyses of the KORUS-AQ data and further show a large contribution from S/IVOCs. Model source attribution of OA in surface air over South Korea indicates one third from domestic anthropogenic emissions, with a large contribution from toluene and xylenes, one third from external anthropogenic emissions, and one third from natural emissions.

Plain Language Summary We have created a new way of understanding how air pollution is formed. We did this by looking at how certain chemicals change when they are exposed to oxygen in the air. We used a computer model of lab experiments to see how these chemicals would react in the atmosphere. The new method is called SOM-VBS. We used this method to study a type of air pollution called secondary organic aerosol that comes from the reaction of oxygen in the air with emissions from both natural and human activities. We found that the new method was able to explain the observations from a field campaign in South Korea better than previous methods. This new understanding can help us figure out where the pollution is coming from. We also found that one third of the pollution comes from human activities in South Korea, one third comes from human activities outside of South Korea, and one third comes from natural sources like plants and wildfires.

1. Introduction

Aerosol particles are of crucial importance for air quality and climate. Organic aerosols (OA) are a major and growing fraction of aerosol mass (Jimenez et al., 2009; Marais et al., 2017). Most of OA is secondary (SOA), produced in the atmosphere from the oxidation of volatile organic compounds (VOCs), but the mechanisms for SOA formation and removal are still poorly understood and model representations are uncertain (Hodzic et al., 2016; Lannuque et al., 2018; Pai et al., 2020).

Validation: J. F. Brewer

Visualization: J. F. Brewer

Writing – original draft: J. F. Brewer

Writing – review & editing: J. F.

Brewer, D. J. Jacob, S. H. Jathar, Y. He, A. Akherati, S. Zhai, D. S. Jo, A. Hodzic, B. A. Nault, J. L. Jimenez, R. J. Park, Y. J. Oak, H. Liao

OA observations made by research aircraft and from surface sites in Korea during the joint Korea-United States Air Quality Study (KORUS-AQ) in May–June 2016 (Crawford et al., 2021) offer some recent insight into this problem. The majority of OA during KORUS-AQ was oxidized OA of anthropogenic origin, with a major contribution from aromatic and low-volatility VOCs (Jordan et al., 2020; Nault et al., 2018). An ensemble of chemical transport models (CTMs) used to simulate the KORUS-AQ conditions was found to underestimate OA on average by 46% relative to the aircraft observations (Park et al., 2021), and to have little predictive capability for surface sites (Choi et al., 2019; Kumar et al., 2021). Previous CTM studies in regions of high anthropogenic emissions similarly found little ability to reproduce observations and a general underestimate (Hodzic et al., 2020; Schroder et al., 2018; Shah et al., 2019).

Simulation of SOA in current CTMs relies on various schemes. The simplest scheme is to co-emit SOA with the parent VOC at a fixed yield (Chin et al., 2002; S. Kim et al., 2015; Pai et al., 2020), or produce it downwind with a fixed timescale for chemical aging (Hodzic & Jimenez, 2011), assuming SOA to be nonvolatile and removed only by deposition. A more process-based scheme is to have SOA gaseous precursors produced from VOC oxidation partition reversibly into the aerosol on the basis of their volatility (Odum et al., 1996), and this is widely implemented in CTMs using the volatility basis set (VBS) parameterization (Ahmadov et al., 2012; Carlton et al., 2010; Dentener et al., 2006; Donahue et al., 2006; Pye et al., 2010; Shrivastava et al., 2011). Yet another scheme is to explicitly describe SOA formation as coupled to the gas-phase kinetic mechanism, though this has been done only for aqueous-phase SOA formation from biogenic isoprene (Fisher et al., 2016; Marais et al., 2016; McNeill et al., 2012) due to the lack of needed data and the large number of different VOCs responsible for anthropogenic SOA formation.

VBS and related SOA formation schemes based on gas-aerosol partitioning of semi-volatile products of VOC oxidation have relied on fitting to chamber observations of time-dependent SOA yields as a function of VOC reacted (Henze et al., 2008; Ng et al., 2007; Pye et al., 2010). Early work did not account properly for losses of SOA and precursors to chamber walls (Zhang et al., 2014), for sustained SOA formation on timescales longer than the chamber experiments (Cappa & Wilson, 2012; Jathar et al., 2015), or for the importance of highly oxidized organic molecules (HOMs) and oligomer condensation (Bianchi et al., 2019; He et al., 2021). Cappa and Wilson (2012) developed the statistical oxidation model (SOM) to account for changing SOA yields and evolving SOA composition over time as a result of complex multi-step chemistry (Jo et al., 2013) and including wall loss effects in chamber data (Matsunaga & Ziemann, 2010). Hodzic et al. (2016) designed such a SOM scheme for application to CTMs, and further improved the representation of anthropogenic SOA by allowing for explicit formation from semi-volatile organic compound (SVOC) and intermediate-volatility organic compound (IVOC) missing from earlier VBS schemes (Ahmadov et al., 2012; Pye et al., 2010). However, when implemented into the CAM-Chem CTM (Tilmes et al., 2019), the scheme still underestimates OA concentrations during KORUS-AQ (Park et al., 2021). More recently, SOM has been coupled with the Two Moment Aerosol Sectional (TOMAS) microphysical model (SOM-TOMAS) to better account for experimental artifacts (e.g., size-dependent wall losses) and the SOA microphysics while fitting to chamber data (Akherati et al., 2020; He et al., 2020).

In this work, we incorporate the Hodzic scheme into the GEOS-Chem CTM and update the aromatic SOA formation terms using SOM-TOMAS. These changes decrease SOA underestimation relative to observations compared with prior versions of GEOS-Chem (Choi et al., 2019; Park et al., 2021). We further update GEOS-Chem to make use of the CEDS emissions inventories, as in Tilmes et al. (2019) and Hodzic et al. (2020), as well as updated KORUS-specific emissions inventories (Woo et al., 2020) in order to best simulate the KORUS-AQ experimental period. We evaluate the scheme with KORUS-AQ observations and show improvement in OA simulation compared to previous VBS schemes implemented in GEOS-Chem (Choi et al., 2019; Pai et al., 2020; Park et al., 2021; Pye et al., 2010), both in terms of fitting the variability of observations and enabling a more process-based representation. From there we examine the role of aromatic VOCs in driving SOA formation over East Asia and the implications for transport of aerosol pollution from China to Korea.

2. SOA Simulation in GEOS-Chem

In this work we compare OA simulations in GEOS-Chem using different OA schemes: the Simple and Complex schemes that represent the standard options in the model, the Hodzic et al. (2016) scheme, and our updated version of the Hodzic scheme, here referred to as SOM-VBS. The schemes are summarized in Figure 1.

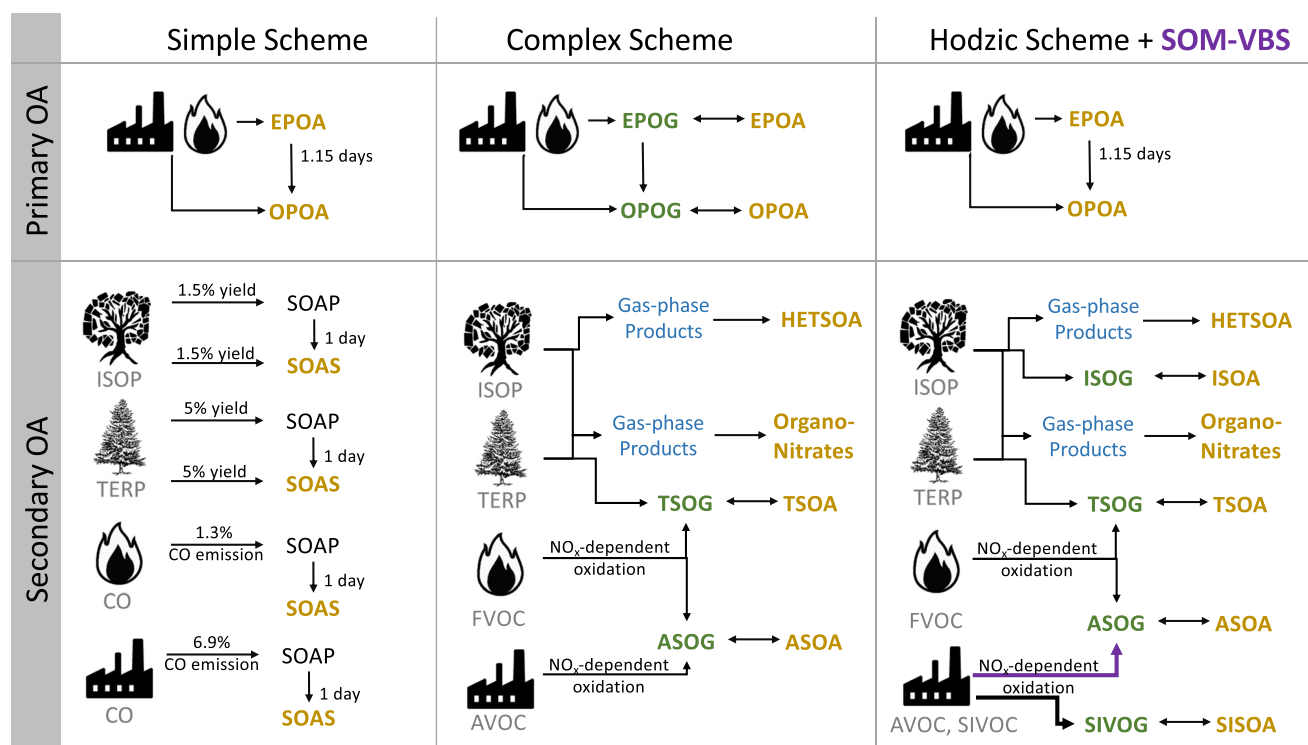


Figure 1. Schematic of the Simple and Complex organic aerosol (OA) schemes in the standard GEOS-Chem model, and our SOM-VBS scheme based on Hodzic et al. (2016). ISOP and TERP refer to isoprene and monoterpene species, respectively, while FVOC represents pyrogenic volatility organic compounds. Anthropogenic (AVOC) species include benzene, toluene, xylene, and various xylene-like aromatic VOCs, while SIVOC include a model representation of semi- and intermediate-volatility organic compounds. Aromatic SOA in the SOM-VBS scheme uses different volatility basis set (VBS) coefficients than in the Complex scheme. Species in orange contribute to OA. This figure is modified from a similar figure presented in Pai et al. (2020).

2.1. Simple Scheme

In the Simple scheme, primary organic aerosol (POA) is handled with two species representing emitted and oxidized POA (EPOA and OPOA, respectively). Both species are directly emitted and EPOA converts to OPOA with a lifetime of 1.15 days (Henze et al., 2008; Pye & Seinfeld, 2010). SOA is nonvolatile and is formed by atmospheric oxidation of tagged precursors with lifetimes of 1 day. These tagged precursors represent different source types and are emitted in proportion to proxy species: CO emissions from wildfires, biofuel, and fossil fuel combustion (Cubison et al., 2011; Hayes et al., 2015; S. Kim et al., 2015) and biogenic emissions of isoprene (S. Kim et al., 2015) and terpenes (Chin et al., 2002).

2.2. Complex Scheme

The Complex scheme combines a VBS algorithm (Pye et al., 2010) with explicit aqueous-phase mechanisms for isoprene SOA (Marais et al., 2016) and nitrate-containing SOA (Fisher et al., 2016). It can be run with POA being either nonvolatile (as in the simple scheme) or semi-volatile (SVPOA). Using the SV POA scheme allows the EPOA to reversibly partition between the gas (EPOG) and aerosol phases. This gas-phase EPOG can oxidize with OH to form low-volatility oxidized primary organic gases which can reversibly partition to the aerosol phase as a function of volatility, seed aerosol abundance, and local conditions (Pai et al., 2020; Pye et al., 2010). The formation of SOA from oxidation of aromatics and terpenes by OH and ozone follows a standard VBS framework (Donahue et al., 2006), and this is also included for isoprene as an option. Different VBS yields are used in the high-NO_x and low-NO_x regimes because the VOC oxidation pathways are different. The branching ratios between high- and low-NO_x oxidation pathways for all SOA precursors are a function of the relative abundances of HO₂ and NO and the rate coefficients of the relevant reactions (Pye & Seinfeld, 2010). Partitioning between the gas and particle phase follows absorptive partitioning theory (Chung & Seinfeld, 2002; Pankow, 1994).

Aerosol precursor yields for the light aromatics (benzene, toluene, and xylene) under high-NO_x conditions are based on three-product fits (298 K effective saturation concentration $C^* = 1, 10, \text{ and } 100 \mu\text{g m}^{-3}$) to chamber

experiment data by Ng et al. (2007). Under low-NO_x conditions, SOA production from these species is treated as a high ($\geq 30\%$) constant yield of nonvolatile products (Henze et al., 2008).

Naphthalene-like IVOC parameterizations for OPOA formation are from Pye and Seinfeld (2010), based on naphthalene chamber experiments by Chan et al. (2009), and are similarly represented in the high-NO_x case with a three-product fit and in the low NO_x case by a constant yield of 73% (Henze et al., 2008; Pye et al., 2010); this parameterization is only used in the SVPOA configuration. More recent research has shown that mobile-source IVOCs, at least, are primarily alkane-like and show significantly different NO_x dependences than a polycyclic aromatic like naphthalene (Lu et al., 2020). Despite the outdated nature of the SVPOA representation in the Complex scheme, recent studies have suggested that it is preferable to the nonvolatile treatment (Pai et al., 2020), and so we use it for the Complex scheme simulations in this paper.

The Complex scheme in GEOS-Chem also includes irreversible aqueous aerosol formation from isoprene oxidation coupled to the gas-phase kinetic mechanism (Marais et al., 2016). The dominant pathways are through the isoprene epoxide and glyoxal, the latter which can also be produced from the oxidation of aromatics (Bates et al., 2021). This aqueous-phase pathway for isoprene SOA formation (HETSOA in Figure 1) can add to the isoprene VBS or supplant it; the default option is to supplant it but here we use both additively. This is of little consequence over South Korea where isoprene is only a small contributor to SOA.

Finally, the Complex scheme includes a mechanism for aqueous-phase formation of organo-nitrate aerosol from gas-phase organic nitrate precursors (Fisher et al., 2016). This mechanism is intended to produce monoterpene nitrates but the standard GEOS-Chem version 12.0.1 used here features the same lumped gas-phase organic nitrate for isoprene and $>C_3$ alkanes, resulting in spurious SOA formation from alkanes. Here we use a separate lumped organic nitrate for $>C_3$ alkanes that does not produce SOA. This decreases organo-nitrate aerosol formation globally by 14% and over the KORUS-AQ domain by 20%.

The Complex scheme has several advantages over the Simple scheme. It links chamber experiments on SOA formation to the model; it makes for realistic precursor apportionment; and it enables predictions of changes in SOA as emissions or meteorological conditions change. However, it is less successful at reproducing atmospheric OA observations than the Simple mechanism—while the Complex scheme can more effectively capture the variability of OA concentrations than the Simple scheme, it systematically underestimates actual OA abundances relative to observations (Pai et al., 2020).

More recent work has shown that the interpretations of chamber experiments used in creation of the Complex scheme underestimated effects of wall loss of the gas-phase low-volatility vapors (Zhang et al., 2014). Other work has illustrated the importance of multigenerational oxidation in SOA formation (Cappa & Wilson, 2012; Hodzic et al., 2016; Jathar et al., 2015), as well as the importance of HOMs and oligomers, all of which can impact aerosol yields as well as volatility of SOA formed from different VOCs (Bianchi et al., 2019; He et al., 2021). Below, we detail a first attempt to incorporate some of these principles into GEOS-Chem (Hodzic et al., 2016) followed by our improvements (SOM-TOMAS scheme).

2.3. The Hodzic et al. (2016) Scheme

Hodzic et al. (2016) updated the VBS of the Complex scheme in GEOS-Chem but this was never included in the standard version of the model. Their VBS used the SOM box model for all SOA precursors (Cappa & Wilson, 2012; Cappa et al., 2013; Jathar et al., 2015), except for the low-volatility VOC families described below. SOM accounts for multi-generational chemistry, including fragmentation and functionalization, and is much better at representing the evolution of SOA yields and O:C ratios over time found in chamber experiments as well as in simulating the dependence of SOA yields on carbon and oxygen numbers of the precursors (Cappa & Wilson, 2012; Cappa et al., 2013). Hodzic et al. (2016) developed SOM box-model parameterizations for individual chamber experiments and NO_x conditions. They then ran them forward under pseudo-atmospheric conditions, fitting the VBS for each parent VOC. They used six volatility bins rather than three to four in Pye et al. (2010). Unlike in Pye et al. (2010), they included a dependence on pre-existing OA, for both high- and low-NO_x regimes. They preserved the isoprene VBS as well as the aqueous isoprene SOA formation mechanism, on the principle that both may additively occur.

Hodzic et al. (2016) also accounted for SOA formation from emitted IVOCs ($C^* = 1 \times 10^4$ – $1 \times 10^6 \mu\text{g m}^{-3}$) and SVOCs ($C^* = 1$ – $1,000 \mu\text{g m}^{-3}$), which have much lower volatility than typical VOCs ($C^* \sim 10^7 \mu\text{g m}^{-3}$).

SVOCs and IVOCs are typically not included in emissions inventories and their composition remains uncertain. The Complex scheme does not explicitly represent SVOCs but instead considers them to be part of POA, and it represents IVOC emissions only as a part of the SVPOA scheme when that option is used (Pye et al., 2010).

Hodzic et al. (2016) set emissions of SVOCs and IVOCs at 60% and 20% of anthropogenic POA and NMVOC emissions, respectively, based on US data (Jathar et al., 2014), and assumed a structure of straight-chain C_{12} - C_{30} n-alkanes (Lee-Taylor et al., 2011). They then used box model simulations with the GECKO-A explicit chemical mechanism at low- and high- NO_x regimes to represent SOA formation from these S/IVOCs, which were then fit to a VBS. More recent work suggests that other S/IVOCs may also contribute to aerosol formation including siloxanes and oxygenated IVOCs (McDonald et al., 2018).

It is important to note that by using a nonvolatile POA scheme and including S/IVOC production of SOA, this scheme is almost certainly double counting some anthropogenic emissions, and more work is necessary to refine POA emissions. It could be argued that Hodzic et al. (2016) treat the nonvolatile fraction of POA as POA, and the semi-volatile fraction as SOA. This treatment is less precise regarding the distinction between “secondary” and “primary” OA than that included in Pye et al. (2010) but is more consistent with how OA measurements by Aerosol Mass Spectrometry (AMS) are taken. The AMS cannot in principle distinguish between semi-volatile oxidized POA and SOA (J. Wang et al., 2021), so maintaining the strong distinction between the two in the OA scheme seems less important.

In addition to these changes to SOA formation, Hodzic et al. (2016) added three loss processes for OA. The first is the inclusion of volatility-dependent dry and wet deposition of gas-phase aerosol precursor species from the VBS (the complex scheme uses Henry's law constants which do not vary by volatility); the second is the photolysis of SOA, which is scaled to the NO_2 photolysis frequency (J_{NO_2}) and loses carbon atoms at a rate of 0.04% of J_{NO_2} ; and the third is an assumed heterogeneous reaction with ozone at the surface of particles at a rate dependent upon both the concentration of ozone and total surface area of OA per volume. These loss rates remain uncertain, but we find that GEOS-Chem is not highly sensitive to them over Korea: the addition of the reaction of ozone and OA decreases OA concentrations by ~10%, and the addition of both the OA photolysis term and the Henry's law changes decrease OA concentrations by ~5%.

2.4. SOM-TOMAS Update to Hodzic et al. (2016) Scheme

Here, we follow the Hodzic et al. (2016) scheme but include an improved representation of aromatic SOA by fitting chamber data to a SOM-TOMAS box model (Akherati et al., 2020; He et al., 2020), and then fitting the box model results to a VBS. Our version of SOM-TOMAS (Akherati et al., 2020; He et al., 2020) includes the formation of HOMs and oligomers from aromatic precursors. In low- NO_x conditions and near-surface temperatures (>253 K; Stolzenburg et al., 2018), peroxy radicals arising from VOC oxidation can auto-oxidize to form HOMs, which generally have very low saturation vapor pressure ($<10^{-4}$ $\mu\text{g}/\text{m}^3$) and are known to contribute to new particle formation and growth (Bianchi et al., 2019; Mehra et al., 2020; Stolzenburg et al., 2018; S. Wang et al., 2017). High-molecular-weight oligomers have also been observed in SOA formation from aromatic compounds under low- NO_x conditions, and are represented in our models with a volume-dependent forward oligomer formation of 10^{-24} cm^3 molecules $^{-1}$ s $^{-1}$ and a first-order dissociation rate of 1.645×10^{-2} s $^{-1}$ (D'Ambro et al., 2018; He et al., 2020, 2022; Sato et al., 2019). HOM yields of 3.4% for low- NO_x simulations were taken from Bianchi et al. (2019). The inclusion of the TOMAS microphysical scheme enables improved representation of both SOA formation microphysics as well as experimental artifacts, including the wall losses of SOA particles and precursor vapors (Akherati et al., 2020; Bilsback et al., 2023; He et al., 2021).

Using SOM-TOMAS, we parameterize our VBS (referred to hereafter as SOM-VBS) using the following three steps:

1. We use SOM-TOMAS to derive OA parameterizations for aromatic species based on chamber experiments detailed in Ng et al. (2007) for benzene and *m*-xylene, and Zhang et al. (2014) for toluene.
2. Using SOM-TOMAS and derived parameters, we perform a combination of four pseudo-atmospheric box-model simulations, accounting for atmospherically representative existing OA background ($1 \mu\text{g m}^{-3}$ for remote regions and $20 \mu\text{g m}^{-3}$ for polluted or urban regions) and NO_x chemical states (high and low- NO_x). We use an atmospherically relevant precursor abundance of 1 pptv for each species, and account for oxidation by typical OH concentration (10^6 molecules cm^{-3}) over time in order to represent SOA formation over the course of 7 days. This approach is similar to methods described earlier in Hodzic et al. (2016) and He et al. (2020).

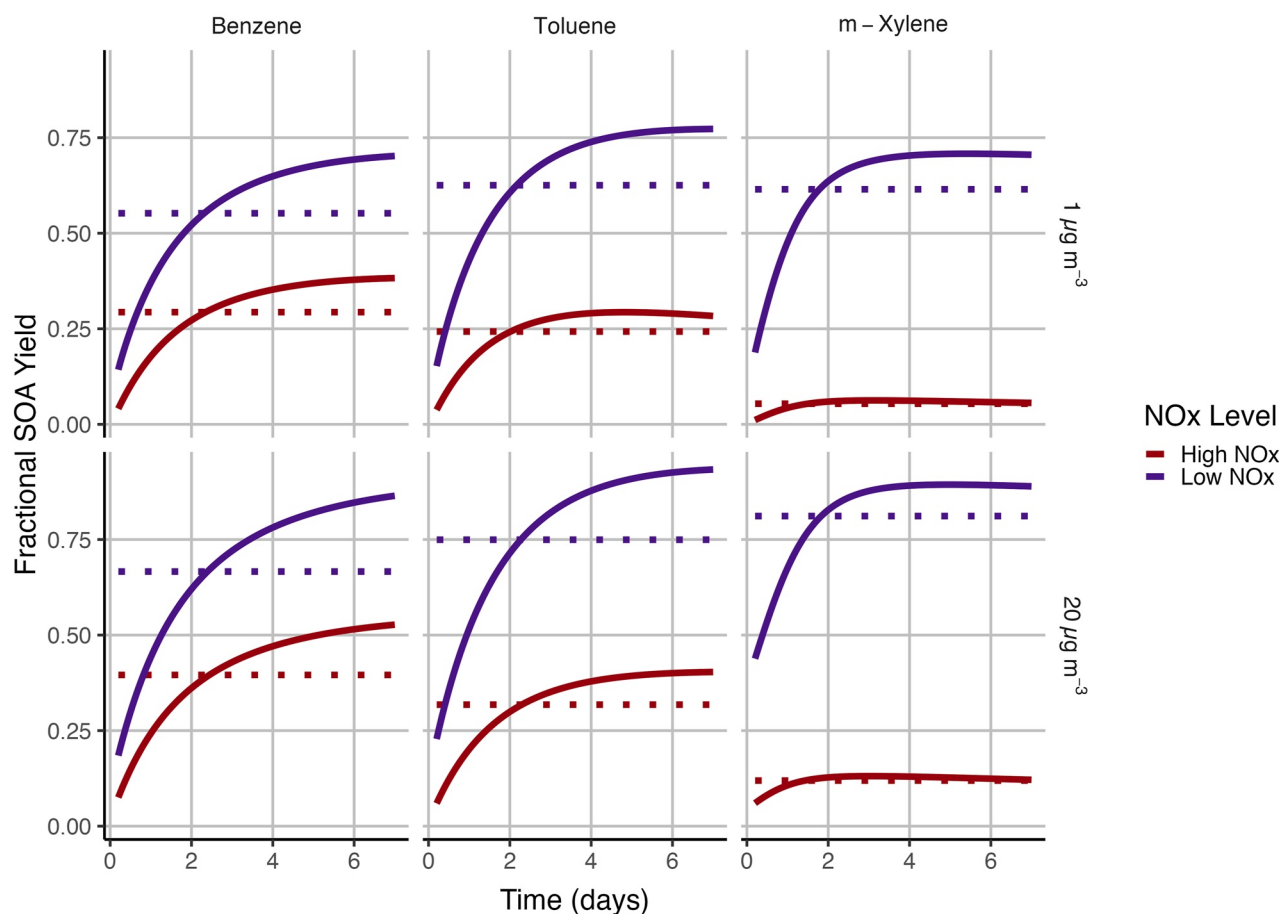


Figure 2. Fractional mass secondary organic aerosol (SOA) yields from the SOM-TOMAS box model scheme (solid lines) and the six-member SOM-volatility basis set (VBS) parameterization scheme (dashed lines) for three aromatic species (benzene, *m*-xylene, and toluene), two NO_x conditions (high- and low-NO_x in red and blue, respectively), and two background organic aerosol concentrations ($C_{\text{OA}} = 1$ and $20 \mu\text{g m}^{-3}$).

- We fit a VBS to the SOM-TOMAS model results for each species (benzene, toluene, *m*-xylene), NO_x condition, and OA backgrounds ($1 \mu\text{g m}^{-3}$ and $20 \mu\text{g m}^{-3}$). We use an iterative nonlinear least-squares solver to optimize the yields of gas-phase SOA precursor products in the VBS to minimize the overall error in total SOA yield.

Surrogate	NO _x ^a	Saturation vapor pressure (C*; $\mu\text{g m}^{-3}$)					
		0.01	0.1	1	10	100	1,000
Benzene	High	0.107	0.177	0.043	0.025	0.291	0.358
Toluene ^b	High	0.130	0.109	0.021	0.026	0.193	0.521
<i>m</i> -Xylene ^c	High	0.028	0.020	0.000	0.079	0.013	0.861
Benzene	Low	0.276	0.258	0.076	0.054	0.125	0.211
Toluene ^b	Low	0.309	0.285	0.109	0.052	0.092	0.153
<i>m</i> -Xylene ^c	Low	0.260	0.247	0.250	0.083	0.066	0.095

^aThe branching ratio between NO_x conditions (high- vs. low-NO_x) is determined by the fraction of organic peroxy (RO₂) radical reacting with NO (Pye et al., 2010). ^bToluene is used as a surrogate to represent the formation of aerosol from toluene, ethyl benzene, *i*-propyl benzene, and *n*-propyl benzene. ^c*m*-Xylene is used as a surrogate to represent the formation of aerosol from *m*, *p*, and *o*-xylenes, and trimethyl benzenes.

Figure 2 shows the VBS performance for each of the three representative aromatic species (benzene, toluene, *m*-xylene) at high- and low-NO_x and high- and low-background OA mass concentration. The corresponding VBS yield parameters for each of the six volatility-classed gas-phase products are given in Table 1. In general, our yields are slightly higher than those used in prior model implementations and considerably higher than those currently used in GEOS-Chem (Hodzic et al., 2016; Pye et al., 2010; Tsimpidi et al., 2010), but share the same general patterns driving higher and lower yields. In particular, the low SOA yields from *m*-xylene under high NO_x conditions shown in Figure 2 are consistent with past studies of *m*-xylene OA yields (Odum et al., 1996; Xu et al., 2015). Toluene here is used as a proxy for other 7-carbon aromatic species, and *m*-xylene is used here as a proxy for other xylene and C₈-aromatic species, an approach commonly used in past analyses (Farina et al., 2010; Hodzic et al., 2016; Jo et al., 2013; Pye et al., 2010).

We do not include an SOA aging scheme in our model, as Hodzic et al. (2020, 2016). Such aging undoubtedly occurs and increases the SOA yield over the first few days of aging, as illustrated in Figure 2, but appears to

have a dampened influence thereafter. Generally speaking, the proper representation of aging in models is uncertain because it is rarely constrained directly to laboratory or ambient data (Heald et al., 2011; Jathar et al., 2016). Not accounting for SOA aging is likely to result in an overestimate of SOA in source regions and an underestimate in remote regions.

3. Simulation of KORUS-AQ Observations

We use the GEOS-Chem CTM version 12.0.1 (Bey et al., 2001) with the different OA schemes of Section 2 to simulate observations from the KORUS-AQ aircraft campaign and surface sites over South Korea (excluding ocean flights) in May–June 2016 (Choi et al., 2019). The simulation is conducted at a nested-grid resolution of $0.25^\circ \times 0.3125^\circ$ over East Asia ($15\text{--}55^\circ\text{N}$, $70\text{--}140^\circ\text{E}$), with dynamic boundary conditions from a global simulation at $2^\circ \times 2.5^\circ$ resolution. Anthropogenic emissions are from the KORUS v5 inventory in South Korea (Woo et al., 2020; http://aisl.konkuk.ac.kr/#/emission_data/korus-aq_emissions), the MEIC inventory in China (Zheng et al., 2021), and the CEDS inventory for the rest of the world (Hoesly et al., 2018). Biogenic VOC emissions are from MEGAN v2.1 (Guenther et al., 2012) and open fire emissions are from GFED 4 (Giglio et al., 2013; Randerson et al., 2012; Werf et al., 2017). POA emissions over East Asia are mainly from fossil fuel combustion, and aromatic VOCs are mainly from fuel and industrial sources. SIVOC emissions are scaled to POA and anthropogenic VOCs as previously mentioned and so are also exclusively anthropogenic, as in Hodzic et al. (2016).

We compare the model to the KORUS-AQ observations by sampling the model output along the aircraft flight tracks and at the surface site locations. We use OA observations from a high-resolution time-of-flight aerosol mass spectrometer (AMS) at a one-minute resolution (Nault et al., 2018) and aromatic gas concentrations from a whole air sampler (Crawford et al., 2021). A positive matrix factorization (PMF) analysis of the AMS data allows us to further separate a hydrocarbon-like organic aerosol (HOA) which we equate to emitted POA in GEOS-Chem, and two oxidized OAs (less-oxidized and more-oxidized; LO-OOA and MO-OOA) which together correspond to the total oxidized OA from GEOS-Chem (i.e., the sum of SOA and oxidized POA) (Nault et al., 2018). Hourly surface observations of particulate organic carbon during KORUS-AQ were taken by a semi-continuous organic carbon/elemental carbon analyzer (SOCEC) (Choi et al., 2019; Crawford et al., 2021).

A comparison of co-located AMS and SOCEC observations at the Olympic Park site shows good agreement between the two measurements and a mass ratio of organic matter (OM) to organic carbon (OC) of roughly 2.0, with some diurnal variation (See Figure S1 in Supporting Information S1). The OM:OC ratio increases during daylight hours and decreases overnight. This increase is consistent with sunlight-dependent production of higher SOA with its higher OM:OC ratio and an increased importance of POA overnight. With the exception of the overnight 1.8 OM:OC ratio, these OM:OC ratios are within the 1.9–2.4 range observed in other regions (Choi et al., 2019; Philip et al., 2014; Turpin & Lim, 2001).

Figure 3 shows the mean vertical profiles of modeled and observed aromatic species over South Korea during KORUS-AQ. To correspond with lumped model definitions, toluene in the model is compared to summed observations of toluene, ethylbenzene, and *i*- and *n*-propylbenzene; xylene in the model is compared to summed *o*-, *m*-, and *p*-xylenes and trimethylbenzenes. The model has minimal bias for benzene but underestimates toluene and xylenes by 30%. This suggests an underestimate of emissions of higher aromatics in GEOS-Chem that may lead to a corresponding low bias in the aromatic SOA contribution.

Figure 4a compares mean vertical profiles of observed and modeled OA concentrations over South Korea grouped in half-kilometer vertical bins. Separation of the KORUS-AQ observation period by meteorological regime (Peterson et al., 2019) gives similar comparison results (Figure S1 in Supporting Information S1). Concentrations exceed $10 \mu\text{g standard m}^{-3}$ near the surface and drop to less than $1 \mu\text{g m}^{-3}$ above 3 km. The GEOS-Chem simulations with the SOM-VBS and Hodzic schemes reproduce the observations while the other schemes are too low as previously found by Park et al. (2021). The SOM-VBS and Hodzic schemes differ only in the treatment of aromatic SOA.

Figure 4b shows the contributions of different OA components to the GEOS-Chem simulations using the SOM-VBS and Complex schemes. POA (mainly oxidized) is similar in both schemes and originates mainly from fuel combustion, but the model representations differ. In the SOM-VBS case it is modeled as nonvolatile POA and in the Complex scheme it is modeled as semi-volatile POA. The Simple scheme does not allow for a comparable decomposition. We see that the OA from the SOM-VBS has major contributions from aromatics

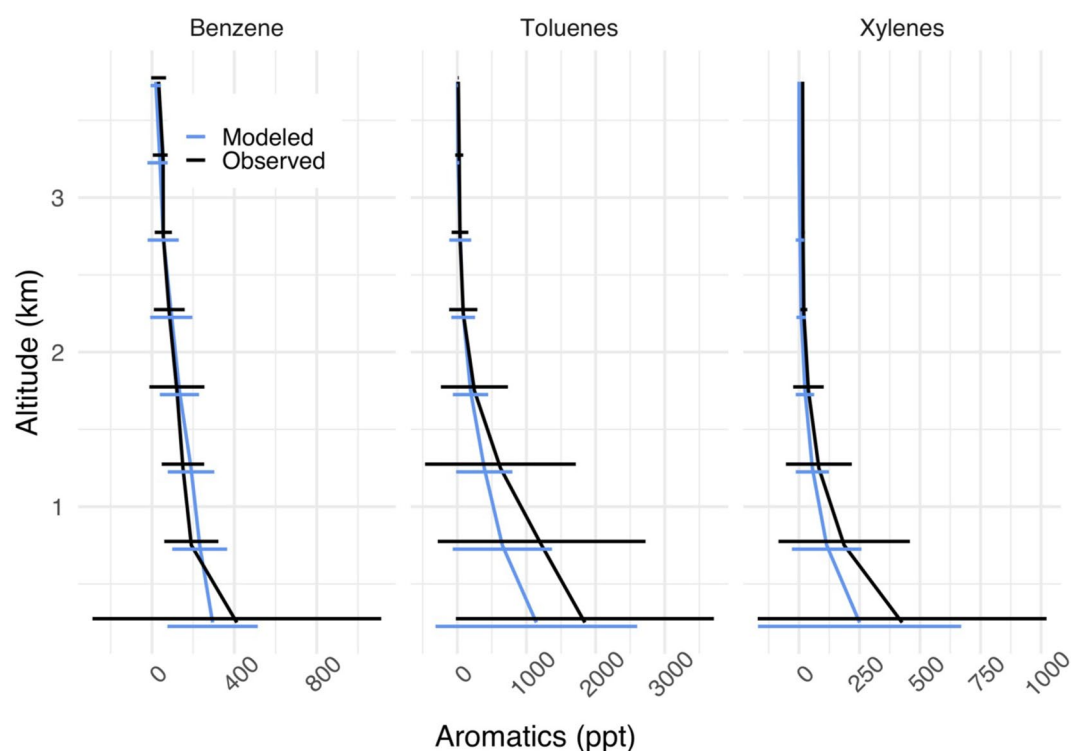


Figure 3. Mean vertical profiles of aromatic volatile organic compounds (VOCs) over Korea during the Korea-United States Air Quality Study (KORUS-AQ) aircraft campaign (May–June 2016). Observations (in black) are compared to the GEOS-Chem model simulation (in blue) along the flight tracks. Horizontal bars indicate one standard deviation. Toluene and xylenes are lumped higher aromatic species to correspond to the GEOS-Chem model mechanism definition (see text). Observations are from the whole air sampler (WAS) instrument (Blake et al., 2003). Note the difference in scales between panels.

and S/IVOCs. The lower concentrations in the Complex scheme are because of a much lower contribution from aromatic SOA and non-accounting of S/IVOCs SOA. Prior analysis of the KORUS data supports a large SOA contribution from aromatic and S/IVOC precursors (Nault et al., 2018).

In their multi-model analysis of the KORUS-AQ data, Park et al. (2021) conclude that “models in general overestimate POA and underestimate SOA throughout the whole campaign.” In GEOS-Chem, this conclusion depends on the interpretation of POA and SOA in the modeling output. Park et al. (2021) map GEOS-Chem POA to the AMS HOA factor and GEOS-Chem SOA to the OOA factors, but the oxidized POA as represented in GEOS-Chem (OPOA) would in fact be more likely to be interpreted by a PMF analysis as OOA (Nault et al., 2018; J. Wang et al., 2021).

Figure 5 thus compares median vertical profiles of HOA and OOA concentrations derived from AMS observations over Korea during KORUS-AQ to the model profiles for different mapping of model components as discussed above. Total OA in the observations is dominated by OOA. We find that model SOA underestimates OOA, as reported by Park et al. (2021) but adding model OPOA produces better agreement. Model POA overestimates HOA by a factor of 4, as reported by Park et al. (2021), but removing model OPOA flips the result to a factor of 2 underestimate. That underestimate could reflect uncertainty in the aging time of EPOA in GEOS-Chem and could also be accounted for by having a small fraction of model OPOA be measured as HOA, as would depend on the extent of oxidation. It is worth noting that Park et al. (2021) found that GEOS-Chem also underestimated OA on the whole during KORUS-AQ; that paper used the Simple scheme which, as shown in Figure 4a, underestimates total OA unlike SOM-VBS.

Figure 6 compares the median diurnal variations of simulated and observed OC aerosol at the six urban surface sites during KORUS-AQ. Aggregated, these observations show no significant diurnal variation, as in previous observations in Beijing in summer (Lin et al., 2009) that were attributed to offset between daytime production of SOA and daytime dilution from mixed layer growth. The SOM-VBS and Hodzic schemes are much better at

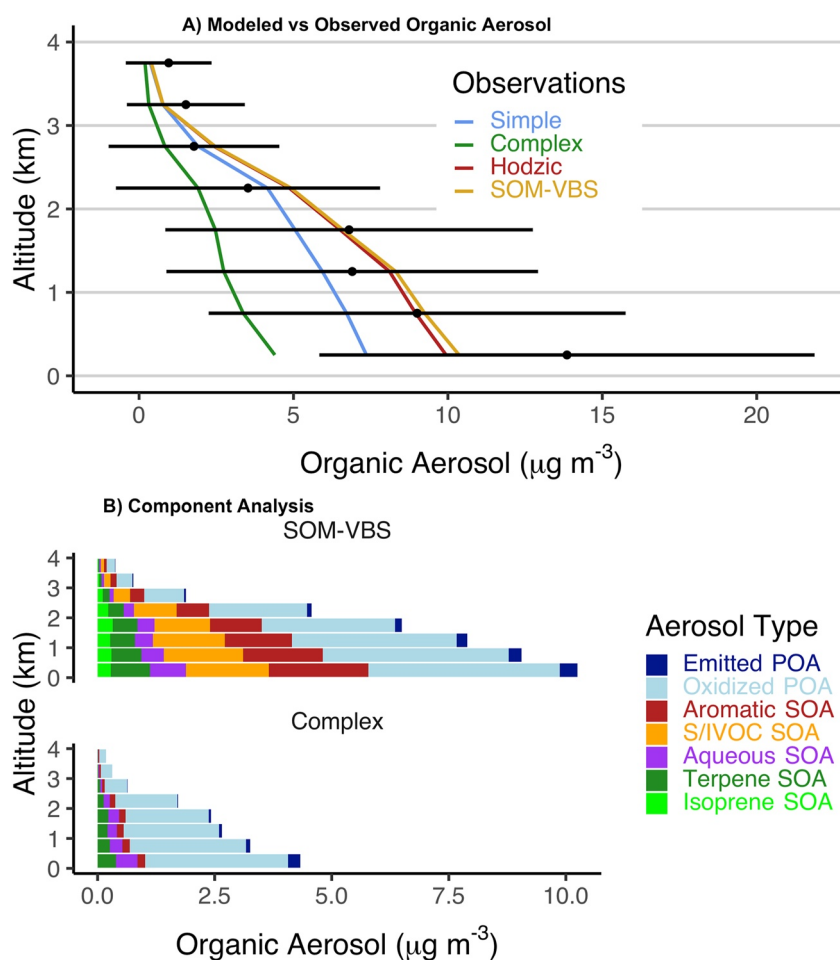


Figure 4. Vertical distribution of organic aerosol (OA) and its GEOS-Chem model components over Korea during Korea-United States Air Quality Study (KORUS-AQ). Panel (a) shows mean vertical profiles of OA observed by the aircraft and simulated by GEOS-Chem with the four alternative OA schemes of Section 2. Horizontal bars for the observations are one standard deviation. Panel (b) shows median abundances of the different OA components simulated by GEOS-Chem for the Complex and SOM-volatility basis set (VBS) schemes.

capturing this offsetting influence because of their photochemical formation of aromatic SOA and S/IVOC SOA, which is consistent with the pattern of OM:OC ratios observed at the Olympic Park site (Figure S2 in Supporting Information S1). The model is too high in the morning, which may reflect delay in mixed layer growth (Travis et al., 2022; Yang et al., 2022). This interplay between photochemical SOA production and mixed layer growth may similarly be the reason for the larger observed variability of concentrations in the morning than at other times of day.

4. Implications for Organic Aerosol Sources and Transboundary Influences

Figure 7 shows the distributions of the different OA components in surface air over the North China Plain and Korea during the KORUS-AQ period. The oxidized POA component dominates everywhere, and as pointed out above it would likely be measured by the AMS instrument as OOA. Aromatic SOA concentrations are similar in Korea and China, but concentrations of POA and S/IVOC SOA are much higher in China. In Korea, aromatics and S/IVOCs together account for 62% of total SOA during May and June. Adding in the contribution from OPOA suggests that 75% of OOA is from aromatics and S/IVOCs, consistent with the analysis of Nault et al. (2018) for Seoul. Over the North China Plain, aromatics and S/IVOCs are responsible for 53% of total SOA in May and June of 2016; OPOA, S/IVOCs, and aromatics are 81% of total OOA (OPOA + SOA), even higher than over Korea.

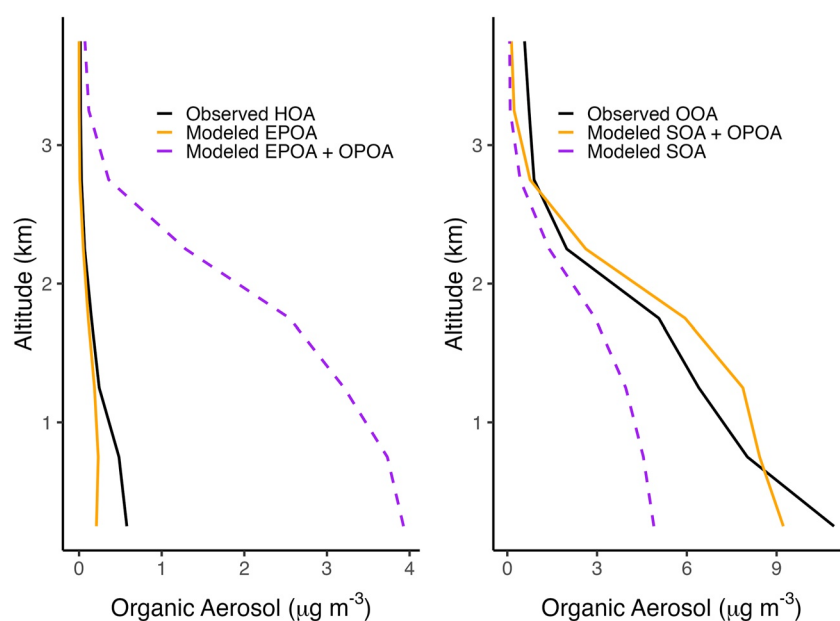


Figure 5. Model comparison to observations of hydrocarbon-like organic aerosol (HOA) and oxidized organic aerosol (OOA) over Korea during Korea-United States Air Quality Study (KORUS-AQ). The figure shows median vertical profiles. Observations are from aerosol mass spectrometer (AMS) and interpreted as HOA and OOA using positive matrix factorization (PMF). Model results are from the SOM-volatility basis set (VBS) scheme. The observations are compared to two alternative mappings of model OA components to HOA and OOA. In the solid orange lines, OOA is represented in GEOS-Chem as the sum of SOA + oxidized primary organic aerosol (POA) while HOA includes emitted POA only. In the dashed purple lines, OOA is only comprised of SOA while HOA includes both emitted and oxidized POA components.

Biogenic SOA accounts for less than 13% of total OA over Korea, China, and southern Japan. This is in remarkable contrast to the United States, where isoprene and terpene SOA dominate the OA aerosol load in summer (Fisher et al., 2016; P. S. Kim et al., 2015; Marais et al., 2016). Some of the conversion of emitted POA to oxidized POA could take place in the aqueous phase (J. Wang et al., 2021), but this is not included here in the aqueous SOA component.

Toluene and xylenes are the most important SOA precursor aromatics in both Eastern China and Korea. For the Eastern China domain of Figure 7 we find that 43%, 42%, and 16% of aromatic SOA are from toluene, xylenes, and benzene respectively; in South Korea, these figures are 45%, 47%, and 8%. Benzene makes a relatively small contribution because of its long lifetime.

Figure 8 shows the total OA concentrations in surface air in South Korea over the KORUS-AQ period, the South Korean background as defined by a simulation without domestic anthropogenic emissions, and the natural background as defined by a simulation without anthropogenic emissions worldwide. Mean OA concentration in South Korea is $8.0 \mu\text{g m}^{-3}$, and controlling domestic anthropogenic emissions could only reduce it by 31% to $5.5 \mu\text{g m}^{-3}$. This South Korean background has a large contribution from external anthropogenic emissions, mainly from China, and controlling these external emissions could reduce OA in South Korea further down to $2.9 \mu\text{g m}^{-3}$, mainly contributed by biogenic sources. The contribution of domestic anthropogenic Korean emissions is largest (up to 50%) in the Seoul and Busan coastal regions, where OA concentrations are highest, and is also largest for aromatic SOA. This is a considerable underestimate compared to the findings of Nault et al. (2018), who suggest that local emissions are responsible for 76%–92% of OA observed over Seoul. This may reflect an underestimate of the emission of OA precursors on our part—Figure 2 shows that GEOS-Chem underestimates both xylene and toluene emissions in Korea, which contribute significantly to SOA formation modeled by Nault et al. (2018). We may also be missing addition S/IVOC emissions. Further evidence for this missing source can be found in the fact that SOM-VBS underestimates OA by the most during the “stagnant period” and “blocking pattern” weather patterns (Figure S1 in Supporting Information S1), when domestic contribution to pollution was at its highest (Choi et al., 2019; Peterson et al., 2019). This missing source is likely to be most important in the highly polluted regions of

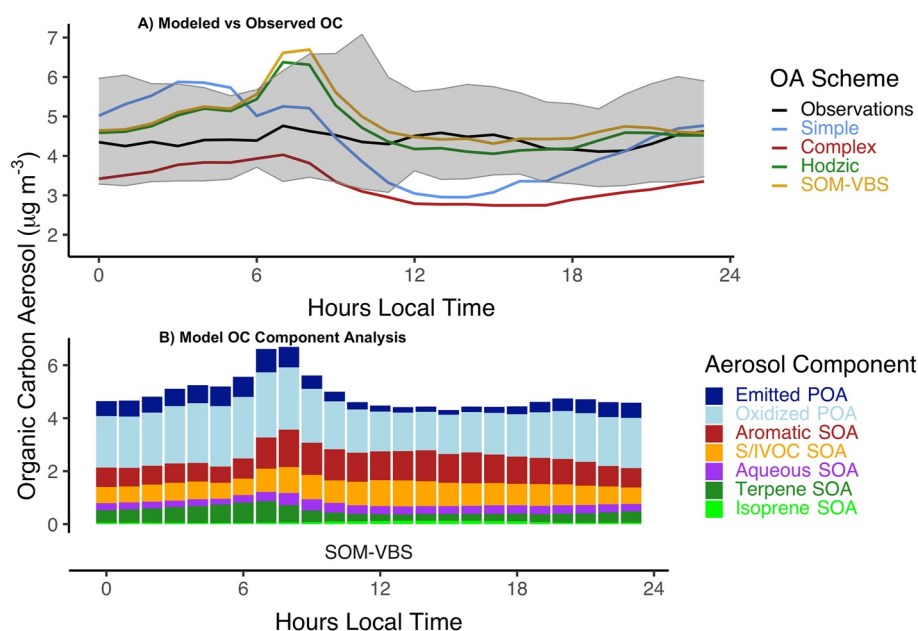


Figure 6. Diurnal variation of organic carbon (OC) aerosol concentrations at urban sites in Korea during the Korea-United States Air Quality Study (KORUS-AQ) campaign (8 May–17 June 2016). The top panel shows the mean hourly concentrations for the ensemble of six urban AirKorea surface sites with OC measurements during KORUS-AQ (Choi et al., 2019): Olympic Park (37.52°N, 127.12°E), Bulkwang (37.62°N, 126.94°E), Daejeon (36.40°N, 127.40°E), Gwangju (35.23°N, 126.94°E), and Ulsan (35.58°N, 129.32°E). Observations (black, with one standard deviation spread in gray) are compared to GEOS-Chem model simulations using the four alternative organic aerosol (OA) schemes. Emitted primary organic aerosol (POA) is converted from organic mass (OM) to OC using an OM:OC mass ratio of 1.4, while other components have an OM:OC ratio of 2.0. The bottom panel shows the contributions of different OA components in the SOM-volatility basis set (VBS) scheme.

Korea (where Nault et al. (2018) focused their efforts); in the rest of Korea, the natural background contribution increases, as shown in Figure 8.

5. Conclusions

We present here an updated volatility basis set (SOM-VBS) for use in global CTMs to better represent the production of SOAs from the oxidation of aromatic precursors. This scheme builds on the OA scheme introduced to GEOS-Chem by Hodzic et al. (2020, 2016). We use SOM-TOMAS to re-examine previous laboratory experiments of aromatic SOA formation to correct the observed aerosol yields for gas and particle wall losses, multiple generations of oxidation, and the formation of HOMs and oligomers. These updated aerosol mass yields are then used to develop a set of VBS parameters that represent SOA formation within a global model framework.

We evaluate our scheme against aircraft and surface observations taken over Korea during the KORUS-AQ field campaign. SOM-VBS can simulate OA abundance and variability better than the default schemes used in GEOS-Chem and confirms the important contribution of aromatic SOA found in previous analyses of the KORUS-AQ data. The Simple and Complex aerosol schemes in GEOS-Chem underproduce this aromatic SOA. We also find a large SOA contribution from semi- and intermediate VOCs (S/IVOCs). The lack of diurnal cycle in OA concentrations observed at surface urban sites during KORUS-AQ supports the importance of the aromatic and S/IVOC SOA produced during daytime.

Our work corrects the previous underestimate of OA found in an intercomparison of all CTMs applied to simulation of the KORUS-AQ data (Park et al., 2021). A conclusion of that intercomparison was that the models overestimate POA and underestimate SOA, but this reflects their attribution of AMS-observed HOA to POA and all oxidized OA factors (OOA) to SOA. In fact, most of model POA is oxidized (OPOA) and would likely be measured as OOA. By defining modeled OOA as SOA + oxidized POA, we find that GEOS-Chem is unbiased in simulating observed OOA concentrations, which account for 95% of total OA.

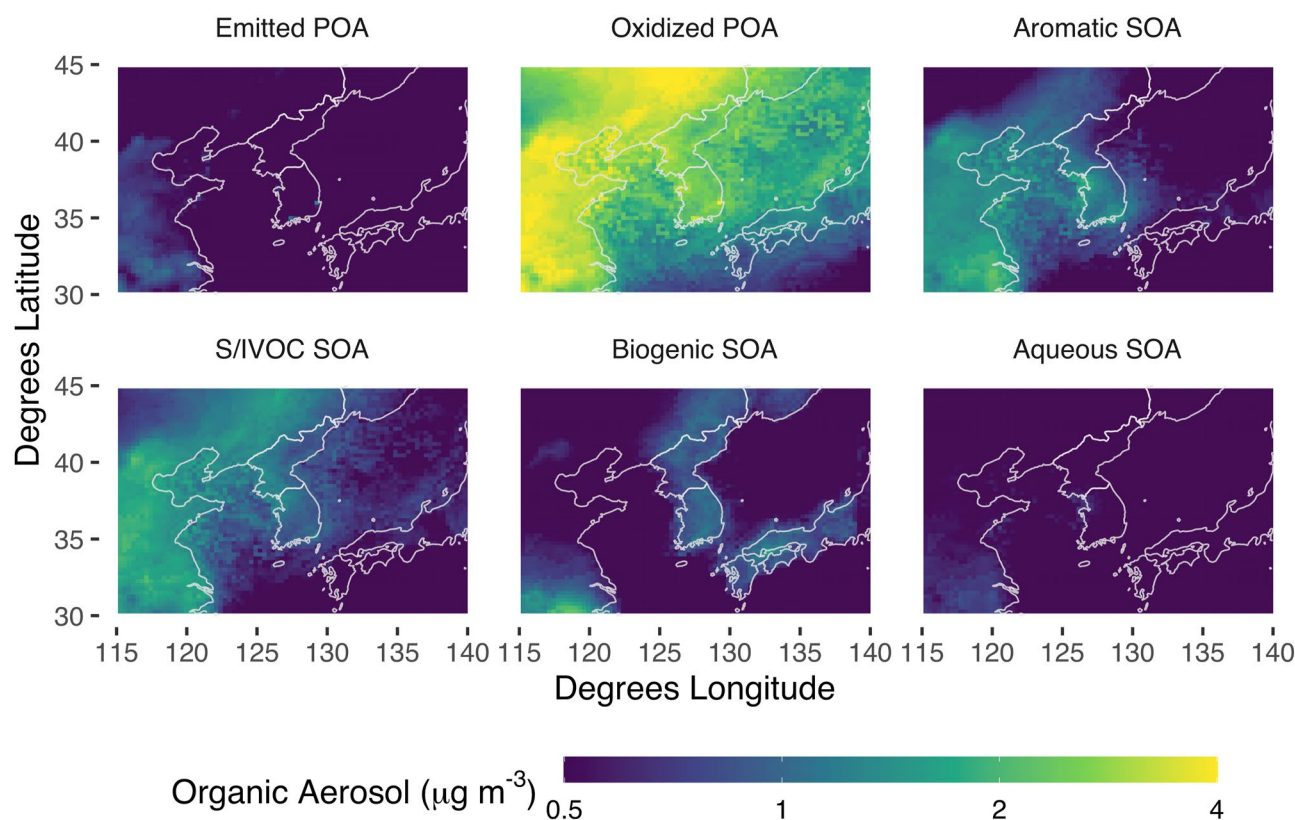


Figure 7. Mean organic aerosol composition in surface air over East Asia during Korea–United States Air Quality Study (KORUS–AQ) (May–June 2016) as simulated by GEOS–Chem with the SOM–volatility basis set (VBS) scheme. The “Biogenic SOA” component includes both isoprene and terpene VBS components. The “Aqueous SOA” component is mainly from isoprene but also includes some production from reactive uptake of glyoxal originating from aromatics and direct emission.

Broader application of our SOM–VBS scheme to interpret sources of OA over South Korea during the KORUS–AQ period finds that anthropogenic sources dominate over the whole region. Oxidized POA is the most important component, followed by aromatic SOA and S/IVOC SOA. Toluene and xylenes are the most important aromatic precursors.

We find that a third of OA in surface air in Korea is from domestic anthropogenic emissions, rising to 50% in the most polluted regions (Seoul and Busan). External anthropogenic emissions, mainly from China, contribute a third of surface OA in Korea, with natural emissions contributing another third. Decreasing aromatic VOC emissions, principally toluene and xylenes, would most effectively decrease the domestic pollution component of OA.

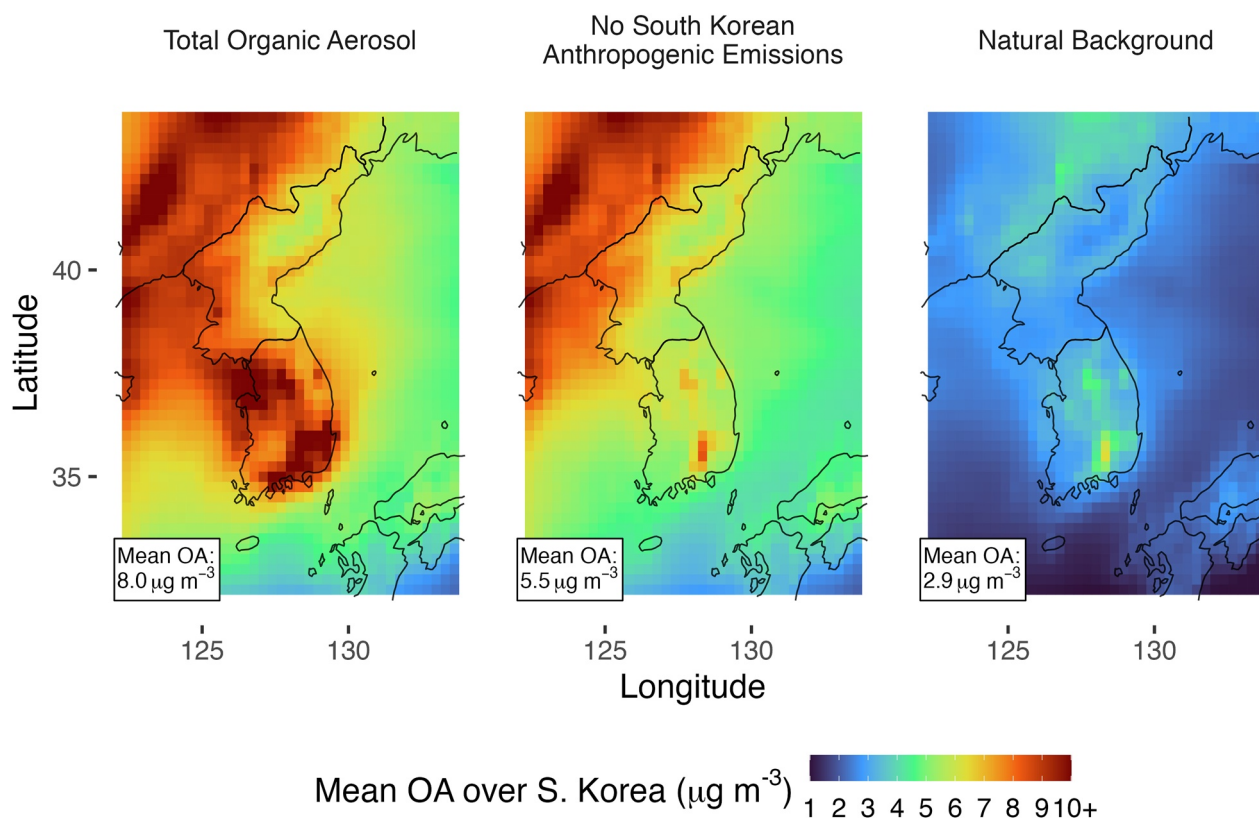


Figure 8. Mean organic aerosol (OA) concentrations in surface air over Korea in May–June 2016 as simulated by GEOS-Chem with the SOM-volatility basis set (VBS) scheme. The left panel shows results from our standard simulation. The middle panel shows results from a simulation with domestic anthropogenic South Korean emissions shut off. The right panel shows the natural background concentrations as determined by a simulation with all anthropogenic emissions shut off. Mean concentrations over South Korea are given inset.

Data Availability Statement

Datasets are available at <https://doi.org/10.7910/DVN/IDWE39> (Brewer et al., 2023).

References

- Ahmadov, R., McKeen, S. A., Robinson, A. L., Bahreini, R., Middlebrook, A. M., Gouw, J. A., et al. (2012). A volatility basis set model for summertime secondary organic aerosols over the eastern United States in 2006. *Journal of Geophysical Research*, *117*(D6). <https://doi.org/10.1029/2011JD016831>
- Akherati, A., He, Y., Coggon, M. M., Koss, A. R., Hodshire, A. L., Sekimoto, K., et al. (2020). Oxygenated aromatic compounds are important precursors of secondary organic aerosol in biomass-burning emissions. *Environmental Science & Technology*, *54*(14), 8568–8579. <https://doi.org/10.1021/acs.est.0c01345>
- Bates, K. H., Jacob, D. J., Li, K., Ivatt, P. D., Evans, M. J., Yan, Y., & Lin, J. (2021). Development and evaluation of a new compact mechanism for aromatic oxidation in atmospheric models. *Atmospheric Chemistry and Physics*, *21*(24), 18351–18374. <https://doi.org/10.5194/acp-21-18351-2021>
- Bey, I., Jacob, D. J., Yantosca, R. M., Logan, J. A., Field, B. D., Fiore, A. M., et al. (2001). Global modeling of tropospheric chemistry with assimilated meteorology: Model description and evaluation. *Journal of Geophysical Research*, *106*(D19), 23073–23095. <https://doi.org/10.1029/2001jd000807>
- Bianchi, F., Kurtén, T., Riva, M., Mohr, C., Rissanen, M. P., Roldin, P., et al. (2019). Highly oxygenated organic molecules (HOM) from gas-phase autoxidation involving peroxy radicals: A key contributor to atmospheric aerosol. *Chemical Reviews*, *119*(6), 3472–3509. <https://doi.org/10.1021/acs.chemrev.8b00395>
- Billsback, K. R., He, Y., Cappa, C. D., Chang, R. Y.-W., Croft, B., Martin, R. V., et al. (2023). Vapors are lost to walls, not to particles on the wall: Artifact-corrected parameters from chamber experiments and implications for global secondary organic aerosol. *Environmental Science & Technology*, *57*(1), 53–63. <https://doi.org/10.1021/acs.est.2c03967>
- Blake, N. J., Blake, D. R., Sive, B. C., Katzenstein, A. S., Meinardi, S., Wingenter, O. W., et al. (2003). The seasonal evolution of NMHCs and light alkyl nitrates at middle to high northern latitudes during TOPSE. *Journal of Geophysical Research*, *108*(D4), 8359. <https://doi.org/10.1029/2001JD001467>
- Brewer, J., Jacob, D. J., Jathar, S. H., He, Y., Akherati, A., Zhai, S., et al. (2023). SOM-VBS evaluation data for KORUS-AQ [Dataset]. Harvard Dataverse. <https://doi.org/10.7910/DVN/IDWE39>

Acknowledgments

This work was funded by the Samsung Advanced Institute of Technology, by the Harvard-NUIST Joint Laboratory for Air Quality and Climate (JLAQC), and by the NASA Atmospheric Composition Campaign Data Analysis and Modeling (ACCDAM) Program. BAN, PC-J, and JLI's contributions were supported by NASA NNX15AT96G and 80NSSC21K1451 and NSF award AGS 2206655.

- Cappa, C. D., & Wilson, K. R. (2012). Multi-generation gas-phase oxidation, equilibrium partitioning, and the formation and evolution of secondary organic aerosol. *Atmospheric Chemistry and Physics*, 12(20), 9505–9528. <https://doi.org/10.5194/acp-12-9505-2012>
- Cappa, C. D., Zhang, X., Loza, C. L., Craven, J. S., Yee, L. D., & Seinfeld, J. H. (2013). Application of the statistical oxidation model (SOM) to secondary organic aerosol formation from photooxidation of C₁₂ alkanes. *Atmospheric Chemistry and Physics*, 13(3), 1591–1606. <https://doi.org/10.5194/acp-13-1591-2013>
- Carlton, A. G., Bhave, P. V., Napelenok, S. L., Edney, E. O., Sarwar, G., Pinder, R. W., et al. (2010). Model representation of secondary organic aerosol in CMAQv4.7. *Environmental Science & Technology*, 44(22), 8553–8560. <https://doi.org/10.1021/es100636q>
- Chan, A. W. H., Kautzman, K. E., Chhabra, P. S., Surratt, J. D., Chan, M. N., Crouse, J. D., et al. (2009). Secondary organic aerosol formation from photooxidation of naphthalene and alkylnaphthalenes: Implications for oxidation of intermediate volatility organic compounds (IVOCs). *Atmospheric Chemistry and Physics*, 9(9), 3049–3060. <https://doi.org/10.5194/acp-9-3049-2009>
- Chin, M., Ginoux, P., Kinne, S., Torres, O., Holben, B. N., Duncan, B. N., et al. (2002). Tropospheric aerosol optical thickness from the GOCART model and comparisons with satellite and sun photometer measurements. *Journal of the Atmospheric Sciences*, 59(3), 23–483. [https://doi.org/10.1175/1520-0469\(2002\)059<0461:taotft>2.0.co;2](https://doi.org/10.1175/1520-0469(2002)059<0461:taotft>2.0.co;2)
- Choi, J., Park, R. J., Lee, H.-M., Lee, S., Jo, D. S., Jeong, J. I., et al. (2019). Impacts of local vs. trans-boundary emissions from different sectors on PM_{2.5} exposure in South Korea during the KORUS-AQ campaign. *Atmospheric Environment*, 203, 196–205. <https://doi.org/10.1016/j.atmosenv.2019.02.008>
- Chung, S. H., & Seinfeld, J. H. (2002). Global distribution and climate forcing of carbonaceous aerosols. *Journal of Geophysical Research*, 107(D19), 4407. <https://doi.org/10.1029/2001JD001397>
- Crawford, J. H., Ahn, J.-Y., Al-Saadi, J., Chang, L., Emmons, L. K., Kim, J., et al. (2021). The Korea–United States Air Quality (KORUS-AQ) field study. *Elementa: Science of the Anthropocene*, 9(1), 00163. <https://doi.org/10.1525/elementa.2020.00163>
- Cubison, M. J., Ortega, A. M., Hayes, P. L., Farmer, D. K., Day, D., Lechner, M. J., et al. (2011). Effects of aging on organic aerosol from open biomass burning smoke in aircraft and laboratory studies. *Atmospheric Chemistry and Physics*, 11(23), 12049–12064. <https://doi.org/10.5194/acp-11-12049-2011>
- D'Ambro, E. L., Schobesberger, S., Zaveri, R. A., Shilling, J. E., Lee, B. H., Lopez-Hilfiker, F. D., et al. (2018). Isothermal evaporation of α -pinene ozonolysis SOA: Volatility, phase state, and oligomeric composition. *ACS Earth and Space Chemistry*, 2(10), 1058–1067. <https://doi.org/10.1021/acsearthspacechem.8b00084>
- Dentener, F., Kinne, S., Bond, T., Boucher, O., Cofala, J., Generoso, S., et al. (2006). Emissions of primary aerosol and precursor gases in the years 2000 and 1750 prescribed data-sets for AeroCom. *Atmospheric Chemistry and Physics*, 6(12), 4321–4344. <https://doi.org/10.5194/acp-6-4321-2006>
- Donahue, N. M., Robinson, A. L., Stanier, C. O., & Pandis, S. N. (2006). Coupled partitioning, dilution, and chemical aging of semivolatile organics. *Environmental Science & Technology*, 40(8), 2635–2643. <https://doi.org/10.1021/es052297c>
- Farina, S. C., Adams, P. J., & Pandis, S. N. (2010). Modeling global secondary organic aerosol formation and processing with the volatility basis set: Implications for anthropogenic secondary organic aerosol. *Journal of Geophysical Research*, 115(D9), D09202. <https://doi.org/10.1029/2009JD013046>
- Fisher, J. A., Jacob, D. J., Travis, K. R., Kim, P. S., Marais, E. A., Chan Miller, C., et al. (2016). Organic nitrate chemistry and its implications for nitrogen budgets in an isoprene- and monoterpene-rich atmosphere: Constraints from aircraft (SEAC⁴RS) and ground-based (SOAS) observations in the southeast US. *Atmospheric Chemistry and Physics*, 16(9), 5969–5991. <https://doi.org/10.5194/acp-16-5969-2016>
- Giglio, L., Randerson, J. T., & Werf, G. R. (2013). Analysis of daily, monthly, and annual burned area using the fourth-generation global fire emissions database (GFED4). *Journal of Geophysical Research: Biogeosciences*, 118(1), 317–328. <https://doi.org/10.1002/jgrg.20042>
- Guenther, A., Jiang, X., Heald, C. L., Sakulyanontvittaya, T., Duhl, T., Emmons, L. K., & Wang, X. (2012). The model of emissions of gases and aerosols from nature version 2.1 (MEGAN2.1): An extended and updated framework for modeling biogenic emissions. *Geoscientific Model Development*, 5(6), 1471–1492. <https://doi.org/10.5194/gmd-5-1471-2012>
- Hayes, P. L., Carlton, A. G., Baker, K. R., Ahmadov, R., Washenfelder, R. A., Alvarez, S., et al. (2015). Modeling the formation and aging of secondary organic aerosols in Los Angeles during CalNex 2010. *Atmospheric Chemistry and Physics*, 15(10), 5773–5801. <https://doi.org/10.5194/acp-15-5773-2015>
- He, Y., Akherati, A., Nah, T., Ng, N. L., Garofalo, L. A., Farmer, D. K., et al. (2021). Particle size distribution dynamics can help constrain the phase state of secondary organic aerosol. *Environmental Science & Technology*, 55(3), 1466–1476. <https://doi.org/10.1021/acs.est.0c05796>
- He, Y., King, B., Pothier, M., Lewane, L., Akherati, A., Mattila, J., et al. (2020). Secondary organic aerosol formation from evaporated biofuels: Comparison to gasoline and correction for vapor wall losses. *Environmental Science: Processes & Impacts*, 22(7), 1461–1474. <https://doi.org/10.1039/D0EM00103A>
- He, Y., Lambe, A. T., Seinfeld, J. H., Cappa, C. D., Pierce, J. R., & Jathar, S. H. (2022). Process-level modeling can simultaneously explain secondary organic aerosol evolution in chambers and flow reactors. *Environmental Science & Technology*, 56(10), 6262–6273. <https://doi.org/10.1021/acs.est.1c08520>
- Heald, C. L., Coe, H., Jimenez, J. L., Weber, R. J., Bahreini, R., Middlebrook, A. M., et al. (2011). Exploring the vertical profile of atmospheric organic aerosol: Comparing 17 aircraft field campaigns with a global model. *Atmospheric Chemistry and Physics*, 11(24), 12673–12696. <https://doi.org/10.5194/acp-11-12673-2011>
- Henze, D. K., Seinfeld, J. H., Ng, N. L., Kroll, J. H., Fu, T. M., Jacob, D. J., & Heald, C. L. (2008). Global modeling of secondary organic aerosol formation from aromatic hydrocarbons: High- vs. low-yield pathways. *Atmospheric Chemistry and Physics*, 16(9), 2405–2420. <https://doi.org/10.5194/acp-8-2405-2008>
- Hodzic, A., Campuzano-Jost, P., Bian, H., Chin, M., Colarco, P. R., Day, D. A., et al. (2020). Characterization of organic aerosol across the global remote troposphere: A comparison of ATom measurements and global chemistry models. *Atmospheric Chemistry and Physics*, 20(8), 4607–4635. <https://doi.org/10.5194/acp-20-4607-2020>
- Hodzic, A., & Jimenez, J. L. (2011). Modeling anthropogenically controlled secondary organic aerosols in a megacity: A simplified framework for global and climate models. *Geoscientific Model Development*, 4(4), 901–917. <https://doi.org/10.5194/gmd-4-901-2011>
- Hodzic, A., Kasibhatla, P. S., Jo, D. S., Cappa, C. D., Jimenez, J. L., Madronich, S., & Park, R. J. (2016). Rethinking the global secondary organic aerosol (SOA) budget: Stronger production, faster removal, shorter lifetime. *Atmospheric Chemistry and Physics*, 25(12), 7917–7941. <https://doi.org/10.5194/acp-16-7917-2016>
- Hoesly, R. M., Smith, S. J., Feng, L., Klimont, Z., Janssens-Maenhout, G., Pitkanen, T., et al. (2018). Historical (1750–2014) anthropogenic emissions of reactive gases and aerosols from the Community Emissions Data System (CEDS). *Geoscientific Model Development*, 11(1), 369–408. <https://doi.org/10.5194/gmd-11-369-2018>
- Jathar, S. H., Cappa, C. D., Wexler, A. S., Seinfeld, J. H., & Kleeman, M. J. (2015). Multi-generational oxidation model to simulate secondary organic aerosol in a 3-D air quality model. *Geoscientific Model Development*, 8(8), 2553–2567. <https://doi.org/10.5194/gmd-8-2553-2015>

- Jathar, S. H., Cappa, C. D., Wexler, A. S., Seinfeld, J. H., & Kleeman, M. J. (2016). Simulating secondary organic aerosol in a regional air quality model using the statistical oxidation model – Part I: Assessing the influence of constrained multi-generational ageing. *Atmospheric Chemistry and Physics*, *16*(4), 2309–2322. <https://doi.org/10.5194/acp-16-2309-2016>
- Jathar, S. H., Gordon, T. D., Hennigan, C. J., Pye, H. O. T., Pouliot, G., Adams, P. J., et al. (2014). Unspecified organic emissions from combustion sources and their influence on the secondary organic aerosol budget in the United States. *Proceedings of the National Academy of Sciences*, *111*(29), 10473–10478. <https://doi.org/10.1073/pnas.1323740111>
- Jimenez, J. L., Canagaratna, M. R., Donahue, N. M., Prevot, A. S. H., Zhang, Q., Kroll, J. H., et al. (2009). Evolution of organic aerosols in the atmosphere. *Science*, *326*(5959), 1525–1529. <https://doi.org/10.1126/science.1180353>
- Jo, D. S., Park, R. J., Kim, M. J., & Spracklen, D. V. (2013). Effects of chemical aging on global secondary organic aerosol using the volatility basis set approach. *Atmospheric Environment*, *81*, 230–244. <https://doi.org/10.1016/j.atmosenv.2013.08.055>
- Jordan, C. E., Crawford, J. H., Beyersdorf, A. J., Eck, T. F., Halliday, H. S., Nault, B. A., et al. (2020). Investigation of factors controlling PM_{2.5} variability across the South Korean Peninsula during KORUS-AQ. *Elementa: Science of the Anthropocene*, *8*, 28. <https://doi.org/10.1525/elementa.424>
- Kim, P. S., Jacob, D. J., Fisher, J. A., Travis, K., Yu, K., Zhu, L., et al. (2015). Sources, seasonality, and trends of southeast US aerosol: An integrated analysis of surface, aircraft, and satellite observations with the GEOS-Chem chemical transport model. *Atmospheric Chemistry and Physics*, *15*(18), 10411–10433. <https://doi.org/10.5194/acp-15-10411-2015>
- Kim, S., Kim, S. Y., Lee, M., Shim, H., Wolfe, G. M., Guenther, A. B., et al. (2015). Impact of isoprene and HONO chemistry on ozone and OVOC formation in a semirural South Korean forest. *Atmospheric Chemistry and Physics*, *15*(8), 4357–4371. <https://doi.org/10.5194/acp-15-4357-2015>
- Kumar, N., Park, R. J., Jeong, J. I., Woo, J.-H., Kim, Y., Johnson, J., et al. (2021). Contributions of international sources to PM_{2.5} in South Korea. *Atmospheric Environment*, *261*, 118542. <https://doi.org/10.1016/j.atmosenv.2021.118542>
- Lannuque, V., Camredon, M., Couvidat, F., Hodzic, A., Valorso, R., Madronich, S., et al. (2018). Exploration of the influence of environmental conditions on secondary organic aerosol formation and organic species properties using explicit simulations: Development of the VBS-GECKO parameterization. *Atmospheric Chemistry and Physics*, *18*(18), 13411–13428. <https://doi.org/10.5194/acp-18-13411-2018>
- Lee-Taylor, J., Madronich, S., Aumont, B., Baker, A., Camredon, M., Hodzic, A., et al. (2011). Explicit modeling of organic chemistry and secondary organic aerosol partitioning for Mexico City and its outflow plume. *Atmospheric Chemistry and Physics*, *11*(24), 13219–13241. <https://doi.org/10.5194/acp-11-13219-2011>
- Lin, P., Hu, M., Deng, Z., Slanina, J., Han, S., Kondo, Y., et al. (2009). Seasonal and diurnal variations of organic carbon in PM_{2.5} in Beijing and the estimation of secondary organic carbon. *Journal of Geophysical Research*, *114*(D2), D00G11. <https://doi.org/10.1029/2008JD010902>
- Lu, Q., Murphy, B. N., Qin, M., Adams, P. J., Zhao, Y., Pye, H. O. T., et al. (2020). Simulation of organic aerosol formation during the CalNex study: Updated mobile emissions and secondary organic aerosol parameterization for intermediate-volatility organic compounds. *Atmospheric Chemistry and Physics*, *20*(7), 4313–4332. <https://doi.org/10.5194/acp-20-4313-2020>
- Marais, E. A., Jacob, D. J., Jimenez, J. L., Campuzano-Jost, P., Day, D. A., Hu, W., et al. (2016). Aqueous-phase mechanism for secondary organic aerosol formation from isoprene: Application to the southeast United States and co-benefit of SO₂ emission controls. *Atmospheric Chemistry and Physics*, *16*(3), 1603–1618. <https://doi.org/10.5194/acp-16-1603-2016>
- Marais, E. A., Jacob, D. J., Turner, J. R., & Mickley, L. J. (2017). Evidence of 1991–2013 decrease of biogenic secondary organic aerosol in response to SO₂ emission controls. *Environmental Research Letters*, *12*(5), 054018. <https://doi.org/10.1088/1748-9326/aa69c8>
- Matsunaga, A., & Ziemann, P. J. (2010). Gas-wall partitioning of organic compounds in a teflon film chamber and potential effects on reaction product and aerosol yield measurements. *Aerosol Science and Technology*, *44*(10), 881–892. <https://doi.org/10.1080/02786826.2010.501044>
- McDonald, B. C., de Gouw, J. A., Gilman, J. B., Jathar, S. H., Akherati, A., Cappa, C. D., et al. (2018). Volatile chemical products emerging as largest petrochemical source of urban organic emissions. *Science*, *359*(6377), 760–764. <https://doi.org/10.1126/science.aag0524>
- McNeill, V. F., Woo, J. L., Kim, D. D., Schwieter, A. N., Wannell, N. J., Sumner, A. J., & Barakat, J. M. (2012). Aqueous-phase secondary organic aerosol and organosulfate formation in atmospheric aerosols: A modeling study. *Environmental Science & Technology*, *46*(15), 8075–8081. <https://doi.org/10.1021/es3002986>
- Mehra, A., Wang, Y., Krechmer, J. E., Lambe, A., Majluf, F., Morris, M. A., et al. (2020). Evaluation of the chemical composition of gas- and particle-phase products of aromatic oxidation. *Atmospheric Chemistry and Physics*, *20*(16), 9783–9803. <https://doi.org/10.5194/acp-20-9783-2020>
- Nault, B. A., Campuzano-Jost, P., Day, D. A., Schroder, J. C., Anderson, B., Beyersdorf, A. J., et al. (2018). Secondary organic aerosol production from local emissions dominates the organic aerosol budget over Seoul, South Korea, during KORUS-AQ. *Atmospheric Chemistry and Physics*, *18*(24), 17769–17800. <https://doi.org/10.5194/acp-18-17769-2018>
- Ng, N. L., Kroll, J. H., Chan, A. W. H., Chhabra, P. S., Flagan, R. C., & Seinfeld, J. H. (2007). Secondary organic aerosol formation from m-xylene, toluene, and benzene. *Atmospheric Chemistry and Physics*, *7*, 4085–4126. <https://doi.org/10.5194/acp-7-3909-2007>
- Odum, J. R., Hoffmann, T., Bowman, F., Collins, D., Flagan, R. C., & Seinfeld, J. H. (1996). Gas/particle partitioning and secondary organic aerosol yields. *Environmental Science & Technology*, *30*(8), 2580–2585. <https://doi.org/10.1021/es950943+>
- Pai, S. J., Heald, C. L., Pierce, J. R., Farina, S. C., Marais, E. A., Jimenez, J. L., et al. (2020). An evaluation of global organic aerosol schemes using airborne observations. *Atmospheric Chemistry and Physics*, *20*(5), 2637–2665. <https://doi.org/10.5194/acp-20-2637-2020>
- Pankow, J. F. (1994). An absorption model of gas/particle partitioning of organic compounds in the atmosphere. *Atmospheric Environment*, *28*(2), 185–188. [https://doi.org/10.1016/1352-2310\(94\)90093-0](https://doi.org/10.1016/1352-2310(94)90093-0)
- Park, R. J., Oak, Y. J., Emmons, L. K., Kim, C.-H., Pfister, G. G., Carmichael, G. R., et al. (2021). Multi-model intercomparisons of air quality simulations for the KORUS-AQ campaign. *Elementa: Science of the Anthropocene*, *9*(1), 00139. <https://doi.org/10.1525/elementa.2021.00139>
- Peterson, D. A., Hyer, E. J., Han, S.-O., Crawford, J. H., Park, R. J., Holz, R., et al. (2019). Meteorology influencing springtime air quality, pollution transport, and visibility in Korea. *Elementa: Science of the Anthropocene*, *7*(1), 57. <https://doi.org/10.1525/elementa.395>
- Philip, S., Martin, R. V., Pierce, J. R., Jimenez, J. L., Zhang, Q., Canagaratna, M. R., et al. (2014). Spatially and seasonally resolved estimate of the ratio of organic mass to organic carbon. *Atmospheric Environment*, *87*, 34–40. <https://doi.org/10.1016/j.atmosenv.2013.11.065>
- Pye, H. O. T., Chan, A. W. H., Barkley, M. P., & Seinfeld, J. H. (2010). Global modeling of organic aerosol: The importance of reactive nitrogen (NO_x and NO₃). *Atmospheric Chemistry and Physics*, *10*(22), 11261–11276. <https://doi.org/10.5194/acp-10-11261-2010>
- Pye, H. O. T., & Seinfeld, J. H. (2010). A global perspective on aerosol from low-volatility organic compounds. *Atmospheric Chemistry and Physics*, *10*(9), 4377–4401. <https://doi.org/10.5194/acp-10-4377-2010>
- Randerson, J. T., Chen, Y., Werf, G. R., Rogers, B. M., & Morton, D. C. (2012). Global burned area and biomass burning emissions from small fires. *Journal of Geophysical Research*, *117*(G4). <https://doi.org/10.1029/2012JG002128>

- Sato, K., Fujitani, Y., Inomata, S., Morino, Y., Tanabe, K., Hikida, T., et al. (2019). A study of volatility by composition, heating, and dilution measurements of secondary organic aerosol from 1,3,5-trimethylbenzene. *Atmospheric Chemistry and Physics*, 19(23), 14901–14915. <https://doi.org/10.5194/acp-19-14901-2019>
- Schroder, J. C., Campuzano-Jost, P., Day, D. A., Shah, V., Larson, K., Sommers, J. M., et al. (2018). Sources and secondary production of organic aerosols in the northeastern United States during WINTER. *Journal of Geophysical Research: Atmospheres*, 123(14), 7771–7796. <https://doi.org/10.1029/2018JD028475>
- Shah, V., Jaeglé, L., Jimenez, J. L., Schroder, J. C., Campuzano-Jost, P., Campos, T. L., et al. (2019). Widespread pollution from secondary sources of organic aerosols during winter in the northeastern United States. *Geophysical Research Letters*, 46(5), 2974–2983. <https://doi.org/10.1029/2018GL081530>
- Shrivastava, M., Fast, J., Easter, R., Gustafson, W. I., Zaveri, R. A., Jimenez, J. L., et al. (2011). Modeling organic aerosols in a megacity: Comparison of simple and complex representations of the volatility basis set approach. *Atmospheric Chemistry and Physics*, 11(13), 6639–6662. <https://doi.org/10.5194/acp-11-6639-2011>
- Stolzenburg, D., Fischer, L., Vogel, A. L., Heinrich, M., Scherhag, M., Simon, M., et al. (2018). Rapid growth of organic aerosol nanoparticles over a wide tropospheric temperature range. *Proceedings of the National Academy of Sciences*, 115(37), 9122–9127. <https://doi.org/10.1073/pnas.1807604115>
- Tilmes, S., Hodzic, A., Emmons, L. K., Mills, M. J., Gettelman, A., Kinnison, D. E., et al. (2019). Climate forcing and trends of organic aerosols in the Community Earth System model (CESM2). *Journal of Advances in Modeling Earth Systems*, 11(12), 4323–4351. <https://doi.org/10.1029/2019MS001827>
- Travis, K. R., Crawford, J. H., Chen, G., Jordan, C. E., Nault, B. A., Kim, H., et al. (2022). Limitations in representation of physical processes prevent successful simulation of PM_{2.5} during KORUS-AQ. *Atmospheric Chemistry and Physics*, 22(12), 7933–7958. <https://doi.org/10.5194/acp-22-7933-2022>
- Tsimpidi, A. P., Karydis, V. A., Zavala, M., Lei, W., Molina, L., Ulbrich, I. M., et al. (2010). Evaluation of the volatility basis-set approach for the simulation of organic aerosol formation in the Mexico City metropolitan area. *Atmospheric Chemistry and Physics*, 22(2), 525–546. <https://doi.org/10.5194/acp-10-525-2010>
- Turpin, B. J., & Lim, H.-J. (2001). Species contributions to PM_{2.5} mass concentrations: Revisiting common assumptions for estimating organic mass. *Aerosol Science and Technology*, 35(1), 602–610. <https://doi.org/10.1080/02786820119445>
- Wang, J., Ye, J., Zhang, Q., Zhao, J., Wu, Y., Li, J., et al. (2021). Aqueous production of secondary organic aerosol from fossil-fuel emissions in winter Beijing haze. *Proceedings of the National Academy of Sciences*, 118(8), e2022179118. <https://doi.org/10.1073/pnas.2022179118>
- Wang, S., Wu, R., Berndt, T., Ehn, M., & Wang, L. (2017). Formation of highly oxidized radicals and multifunctional products from the atmospheric oxidation of alkylbenzenes. *Environmental Science & Technology*, 51(15), 8442–8449. <https://doi.org/10.1021/acs.est.7b02374>
- Werf, G. R., Randerson, J. T., Giglio, L., Leeuwen, T. T., Chen, Y., Rogers, B. M., et al. (2017). Global fire emissions estimates during 1997–2016. *Earth System Science Data*, 9(2), 697–720. <https://doi.org/10.5194/essd-9-697-2017>
- Woo, J.-H., Kim, Y., Kim, H.-K., Choi, K.-C., Eum, J.-H., Lee, J.-B., et al. (2020). Development of the CREATE inventory in support of integrated climate and air quality modeling for Asia. *Sustainability*, 12(19), 7930. <https://doi.org/10.3390/su12197930>
- Xu, J., Griffin, R. J., Liu, Y., Nakao, S., & Cocker, D. R. (2015). Simulated impact of NO_x on SOA formation from oxidation of toluene and m-xylene. *Atmospheric Environment*, 101, 217–225. <https://doi.org/10.1016/j.atmosenv.2014.11.008>
- Yang, L. H., Jacob, D. J., Colombi, N. K., Zhai, S., Bates, K. H., Shah, V., et al. (2022). Tropospheric NO₂ vertical profiles over South Korea and their relation to oxidant chemistry: Implications for geostationary satellite retrievals and the observation of NO₂ diurnal variation from space. *Atmospheric Chemistry and Physics*, 23, 2465–2481. <https://doi.org/10.5194/egusphere-2022-1309>
- Zhang, X., Cappa, C. D., Jathar, S. H., McVay, R. C., Ensberg, J. J., Kleeman, M. J., & Seinfeld, J. H. (2014). Influence of vapor wall loss in laboratory chambers on yields of secondary organic aerosol. *Proceedings of the National Academy of Sciences*, 111(16), 5802–5807. <https://doi.org/10.1073/pnas.1404727111>
- Zheng, B., Cheng, J., Geng, G., Wang, X., Li, M., Shi, Q., et al. (2021). Mapping anthropogenic emissions in China at 1 km spatial resolution and its application in air quality modeling. *Science Bulletin*, 66(6), 612–620. <https://doi.org/10.1016/j.scib.2020.12.008>